Structural cell biology with smart STED microscopy

Laurell F. Kessler[a], Enya S. Berrevoets[b], Ashwin Balakrishnan[a], Ellen K. Okuda[c], Michaela Müller-McNicoll[c,d], Bernd Rieger[b], Sjoerd Stallinga[b], Mike Heilemann*[a]

[a]Institute of Physical and Theoretical Chemistry, Goethe University Frankfurt, Frankfurt, Germany; [b]Department of Imaging Physics, Delft University of Technology, Delft, The Netherlands; [c]Institute of Molecular Biosciences, Goethe University, Frankfurt am Main, Germany; [s]Max Planck Institute for Biophysics, Frankfurt am Main, Germany

*heilemann@chemie.uni-frankfurt.de, phone +49 69 798 29424, www.smb.uni-frankfurt.de

ABSTRACT

We developed a fully-automated smart fluorescence microscopy workflow that combines fast confocal microscopy, morphological object screening, event-triggered and targeted 3D super-resolution STED microscopy and quantitative image analysis. This workflow was tailored to search for and identify rare objects or events in cells, and to subsequently direct the full performance of the microscope towards a nanoscale characterization of these objects. Using this workflow, we measured the 3D nano-morphology of paraspeckles, a phase-separated membrane-less organelle (MLO) located in the nucleus of eukaryotic cells. Furthermore, we applied this workflow to detect cell organelle contact sites in living cells. This smart microscopy approach is resource-efficient, enables targeted and high-throughput characterization of rare objects and events, and is transferable to a large variety of cellular structures.

Keywords: smart microscopy, super-resolution microscopy, live-cell microscopy, STED, membrane-less organelles, organelle contact sites

1. INTRODUCTION

Super-resolution fluorescence microscopy has evolved into a powerful tool for cell biology research [1]. A remaining challenge is that most super-resolution imaging methods are slow, such that high-throughput imaging requires long acquisition times, and the temporal resolution in live cell experiments is limited. One strategy to bypass these limitations are attention-sensitive or event-triggered microscopy workflows, which are grouped under the term 'smart microscopy' [2,3]. Several experimental concepts have been reported that integrate different types of super-resolution microscopy into smart microscopy workflows, such as single-molecule localization microscopy [4,5], stimulated-emission depletion (STED) microscopy [6–8] and structured illumination microscopy (SIM) [9].

Here, we report an automated super-resolution imaging and analysis workflow that integrates fast confocal microscopy on a large field-of-view, morphological object screening, targeted 3D STED microscopy and quantitative image analysis [10]. This workflow enables resource-efficient STED microscopy, combining high-throughput, fast and low-resolution screening of large samples or of a large number of targets with high-performance imaging triggered by the occurrence of an event in space or in time. We apply this workflow to (i) high-throughput super-resolution imaging of a membrane-less organelle in the cell nucleus, and for (ii) live-cell imaging triggered by the occurrence of a membrane contact between mitochondria and the endoplasmic reticulum (ER).

Single Molecule Spectroscopy and Superresolution Imaging XIX, edited by Rainer Erdmann, Mike Heilemann, Felix Koberling, Proc. of SPIE Vol. 13858, 1385806
2026 Published by SPIE · 1605-7422 · doi: 10.1117/12.3084913

2. RESULTS

2.1 An experimental workflow for event-triggered STED microscopy

The smart microscopy workflow was realized on a commercial STED microscope that can be operated in both confocal imaging mode, enabling fast scanning of large volumes, and high-performance 3D STED, enabling high-resolution ultra-structural imaging of small volumes. Automated image analysis is used to identify objects that are subjected to targeted 3D super-resolution STED microscopy (**Figure 1**) [10]. This procedure enables the unsupervised acquisition of a large amount of 3D super-resolution data of target objects from entire cell volumes.

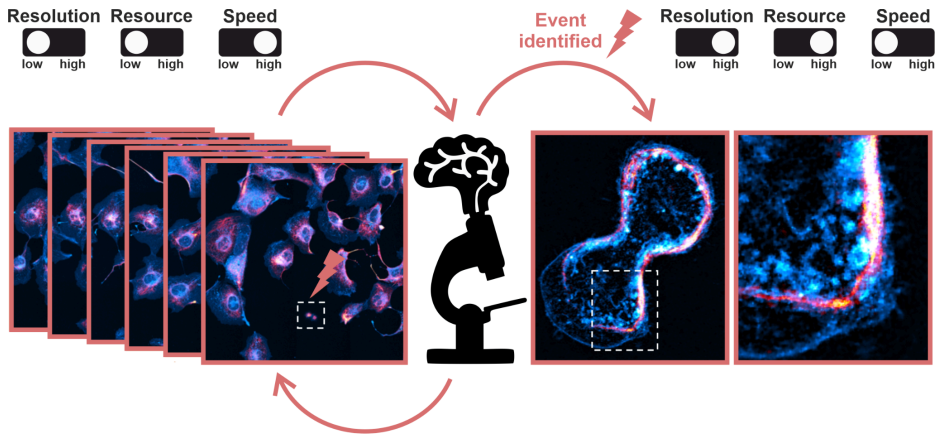

Figure 1: The principle of event-triggered 3D STED microscopy. Fast confocal microscopy (left) enables visualizing large field-of-views. The occurrence of a pre-defined event (box) triggers the microscope to switch to high-resolution 3D STED microscopy of a selected target (right).

2.2 Smart STED microscopy unravels the ultrastructure of paraspeckles *in situ*

We applied the smart microscopy workflow to visualize the ultrastructure of paraspeckles, a membrane-less organelle that occurs in the nucleus of eukaryotic cells [11,12]. For that purpose, we employed RNA fluorescence in-situ hybridization (RNA FISH) to fluorophore-label a central structural element of paraspeckles, the architectural RNA *NEAT1*, at different positions (**Figure 2A**) [10]. This allowed identifying paraspeckles in 3D confocal microscopy in the cell nucleus (**Figure 2B**). We next employed the smart microscopy workflow and conducted fast confocal microscopy of large volumes, identified objects upon their size and shape, and targeted these objects to 3D super-resolution STED microscopy in small volumes (**Figure 2C**). With that approach, it was possible to record a large number of paraspeckles (> 10.000) in super-resolution mode with an about two orders faster acquisition time as compared to whole-cell 3D STED imaging only. This enabled particle sorting and grouping (**Figure 2Di**) and subsequently the extraction of essential structural features such as the morphology and the coarse conformation of the architectural RNA *NEAT1* in paraspeckles (**Figure 2Dii**).

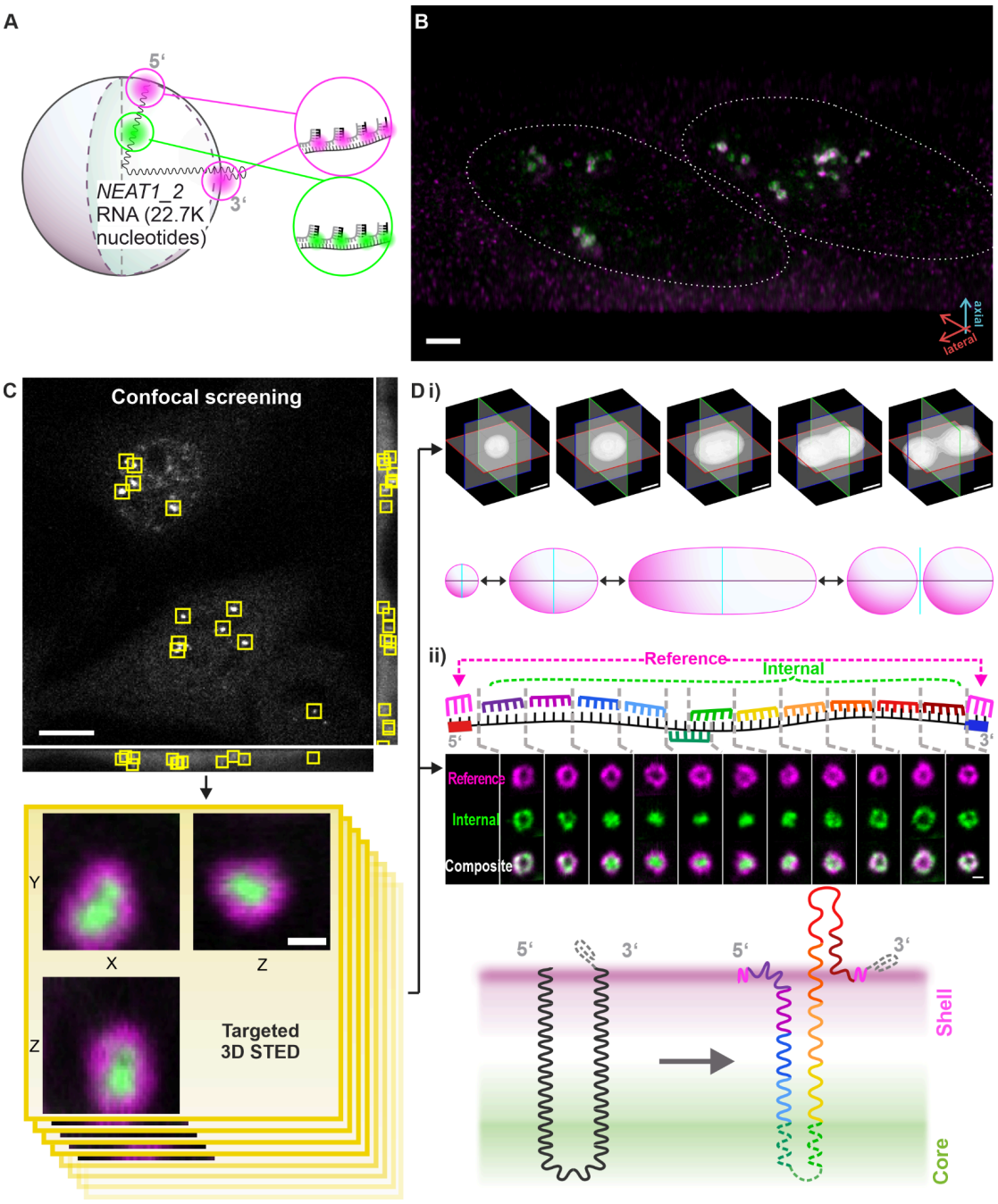

Figure 2: Smart microscopy of paraspeckles in HeLa cells. A The architectural RNA *NEAT1* of paraspeckles was labeled at different positions using RNA-FISH. **B** Two-color 3D confocal microscopy of paraspeckles in a HeLa cell. **C** Fast confocal imaging of a large field-of-view and automated object detection identified targets for 3D STED microscopy. **D** Targeted 3D STED microscoppüy unraveled (i) the morphological space of paraspeckles and (ii) the distribution and coarse conformation of NEAT1 inside paraspeckles. Scale bars are 2 µm (B), 10 µm (C, confocal image) and 300 nm (STED images) (Adapted from Berrevoets et al. [10] under the terms of CC BY 4.0.

2.3 Live-cell smart STED microscopy of organelle contact sites

We used the smart microscopy workflow to track rare events in living cells. For a demonstration, we targeted transient contacts of the endoplasmic reticulum (ER) and mitochondria. For this, we used a cell line expressing calreticulin-KDEL-HaloTag7 targetable with fluorophore-conjugated HaloTag ligands to visualize the ER (**Figure 3**, red) and PKmito ORANGE (PKMO) [13] (**Figure 3**, green), a lipophilic and cationic dye assembling in the cristae of mitochondria. Using the overlapping (yellow) regions of both targets in a confocal screened volume (**Figure 3A**) as an event trigger, we were able to automatically identify potential dynamically formed ER-mitochondria contact sites (ERMCS) in living cells. By measuring small volumes around the identified region, the measurement speed could be drastically accelerated, and the potential ERMCS were visualized using volumetric STED (**Figure 3B**). This highlights the potential of smart STED microscopy in live-cell imaging of rare events, which provided ultra-structural information on ER-mitochondria contact sites.

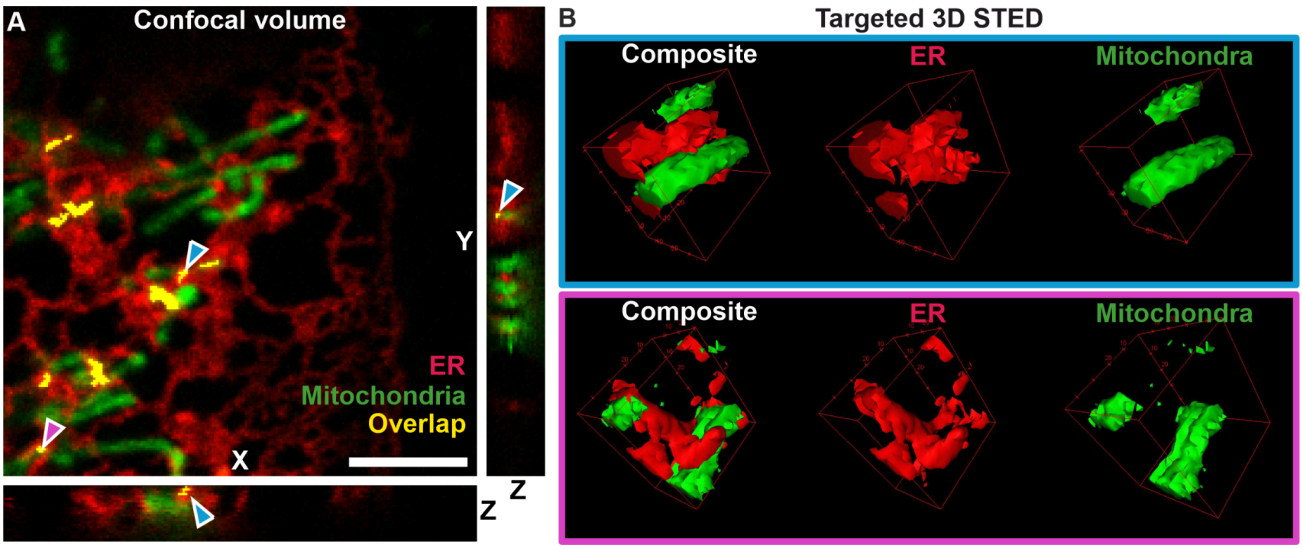

Figure 3. Event-triggered 3D STED microscopy in living cells. A Fast 3D confocal microscopy of the endoplasmic reticulum (ER, red) and mitochondria (green) in living U-2 OS cells. Overlapping structures are highlighted in yellow. **B** Two selected events in **A** (arrows) were identified by a colocalization signal and targeted by 3D STED imaging.

3. CONCLUSION AND OUTLOOK

Smart microscopy using event triggering is a resource-efficient strategy to direct the full performance of high-resolution microscopes to pre-defined cellular objects. This bypasses the slow acquisition of many super-resolution methods, and thus enables fast live-cell imaging and high-throughput collection of relevant imaging data. Employing weak-affinity protein labels, which transiently and repeatedly bind to their target [14], would bypass photobleaching and extend observation times in living cells [15–18]. The integration of neural networks would further increase the imaging speed and reduce the phototoxicity, as previously demonstrated for fast and live-cell STED microscopy of cellular dynamics [19,20]. The combination with other imaging modes, such as phase contrast, further reduces the light-induced stress of cells and enables gentle event-driven microscopy [21].

The approach is transferable to a large variety of biological targets, and would for example allow tracking the ultra-structural organization in bacterial cells [22,23] or the uptake of viruses [24]. Beyond shape and signal overlap, other types of proximity information triggers, such as single-molecule Förster resonance energy transfer (smFRET), could be integrated and used to track the association of biomolecules at single-protein resolution in living cells [25,26].

4. METHODS

All experimental details except live-cell imaging are accessible in the original publication [10].

Sample preparation

U2-OS cells inducibly expressing calreticulin-KDEL-HaloTag7 were seeded onto fibronectin-coated (Sigma-Aldrich, Germany, 0.1% v/v fibronectin human plasma for 30 min) 8-well chambered coverglass (Sarstedt, Germany) at a density of 1×10^4 cells per well. The cells were incubated overnight at 37 °C and 5% CO_2 and were induced the next day with 500 µg/mL doxycycline (Sigma Aldrich, Germany) in cell culture media (Gibco, Life Technologies). Two days post-induction, the cells were incubated for 15 min with 300 nM of HaloTag ligand conjugated to SiR fluorophore (SiR-HTL) and 250 nM of PKmito ORANGE (PKMO). The cells were then washed twice with cell culture media at 37 °C with 5% CO2 and a 5 min waiting time between wash steps.

STED microscopy

STED imaging experiments were conducted with an Abberior Expert Line (Abberior Instruments, Germany). The microscope was equipped with an Olympus IX83 body (Olympus Deutschland GmbH, Germany), a UPLXAPO 60x NA 1.42 oil immersion objective (Olympus Deutschland GmbH, Germany), and three laser sources (561 nm, 640 nm and 775 nm) operating at a repetition rate of 40 MHz.
For volumetric confocal screening, samples were excited with a 561 nm (5.8 µW before objective, 18 kW/cm^2) and 640 nm pulsed excitation laser (1.4 µW before objective, 4.5 kW/cm^2). Fluorescence was collected in the spectral windows of 571 nm to 630 nm (PKMO) and 650 nm to 763 nm (SiR), respectively, using two avalanche photodiodes (APDs). The pinhole was set to 0.81 AU, and scanning was performed with a pixel dwell time of 5 µs and a single line accumulation. A volume of 20 x 20 x 2.5 µm³ was recorded using an isotropic voxel size of 100 nm. Targeted two-color volumetric STED was performed using a 561 nm excitation laser (15 µW before objective, 48 kW/cm^2), a 640 nm excitation laser (10 µW before objective, 32 kW/cm^2), and a 775 nm pulsed depletion laser (35 mW before objective, 110 MW/cm^2) with a 3D top-hat point spread function. The fluorescence was detected 750 ps after every pulse over a time window of 8 ns. Fluorescence was collected in the spectral range of 571-630 nm (PKMO) and 650-763 nm (SiR) using two APDs. The pinhole was set to 0.81 AU, and scanning was performed with a pixel dwell time of 500 ns, single line accumulation, and an isotropic voxel size of 40 nm.
Event-triggering was realized with a custom Python script [10] integrated into *SpecPy*, a Python interface for *Imspector*. To identify potential organelle contact sides, the confocal stacks were blurred using a Gaussian blur of 0.6 voxels and thresholded using the Kapur-Sahoo-Wong Maximum Entropy method. The overlapping volume of the two masked stacks was determined using a bitwise AND operation. Centroid coordinates of overlapping regions exceeding 0.01 µm³ were extracted and used as target coordinates for targeted STED imaging.

Acknowledgements

We thank Julian Kompa and Kai Johnsson (MPI Medical Research, Heidelberg) for kindly providing U2-OS cells stably expressing calreticulin-KDEL-HaloTag7, and Zhixing Chen for providing PKMO. We thank Petra Freund for assistance with cell culture. This work was supported by the Deutsche Forschungsgemeinschaft (DFG, German Research Foundation) through SFB 1177 (project-id: 259130777) (M.H.) and INST 161/1020-1 FUGG (M.H.); ; the SubCellular Architecture of LifE (SCALE) consortium funded by the Goethe University Frankfurt, Germany (M.H., L.F.K., E.K.O., M.M.M.); the GRADE Center SCALE-it (L.F.K.).

REFERENCES

[1] Danial, J.S.H., "Super-resolution microscopy for structural biology," Nature methods 22(8), 1636–1652 (2025).
[2] Mahecic, D., Testa, I., Griffié, J., and Manley, S., "Strategies for increasing the throughput of super-resolution microscopies," Current opinion in chemical biology 51, 84–91 (2019).
[3] Hinderling, L., Heil, H.S., Rates, A., Seidel, P., Gunkel, M., Diederich, B., Guilbert, T., Torro, R., Bouchareb, O., et al., "Smart microscopy: Current implementations and a roadmap for interoperability," in bioRxiv (2025).
[4] Flottmann, B., Gunkel, M., Lisauskas, T., Heilemann, M., Starkuviene, V., Reymann, J., and Erfle, H., "Correlative light microscopy for high-content screening," BioTechniques 55(5), 243–252 (2013).
[5] Gunkel, M., Flottmann, B., Heilemann, M., Reymann, J., and Erfle, H., "Integrated and correlative high-throughput

and super-resolution microscopy," Histochemistry and cell biology 141(6), 597–603 (2014).
[6] Alvelid, J., Damenti, M., Sgattoni, C., and Testa, I., "Event-triggered STED imaging," Nature methods 19(10), 1268–1275 (2022).
[7] Bouchard, C., Wiesner, T., Deschênes, A., Bilodeau, A., Turcotte, B., Gagné, C., and Lavoie-Cardinal, F., "Resolution enhancement with a task-assisted GAN to guide optical nanoscopy image analysis and acquisition," Nature machine intelligence 5(8), 830–844 (2023).
[8] Mol, F.N., and Vlijm, R., "Automated STED nanoscopy for high-throughput imaging of cellular structures," biorxiv;2022.09.29.510126v1, in Biophysics, bioRxiv (2022).
[9] Mahecic, D., Stepp, W.L., Zhang, C., Griffié, J., Weigert, M., and Manley, S., "Event-driven acquisition for content-enriched microscopy," Nature methods 19(10), 1262–1267 (2022).
[10] Berrevoets, E.S., Kessler, L.F., Balakrishnan, A., Okuda, E.K., Müller-McNicoll, M., Rieger, B., Stallinga, S., and Heilemann, M., "Smart 3D super-resolution microscopy reveals the architecture of the RNA scaffold in a nuclear body," Nature communications 16(1), 10689 (2025).
[11] Souquere, S., Beauclair, G., Harper, F., Fox, A., and Pierron, G., "Highly ordered spatial organization of the structural long noncoding NEAT1 RNAs within paraspeckle nuclear bodies," Molecular biology of the cell 21(22), 4020–4027 (2010).
[12] Okuda, E.K., Kessler, L.F., Arnold, B., Riegger, R.J., Hernández Cañás, M.C., Zebrowska, E., Bakisoglu, C., Rudigier, M., Krost, C., et al., "Rapid depletion and super-resolution microscopy reveal dual roles of SRSF5 in coordinating nuclear speckle-paraspeckle crosstalk during cellular stress," Nucleic acids research 53(14), (2025).
[13] Liu, T., Stephan, T., Chen, P., Keller-Findeisen, J., Chen, J., Riedel, D., Yang, Z., Jakobs, S., and Chen, Z., "Multi-color live-cell STED nanoscopy of mitochondria with a gentle inner membrane stain," Proceedings of the National Academy of Sciences of the United States of America 119(52), e2215799119 (2022).
[14] Albertazzi, L., and Heilemann, M., "When Weak Is Strong: A Plea for Low-Affinity Binders for Optical Microscopy," Angewandte Chemie (International ed. in English) 62(35), e202303390 (2023).
[15] Kompa, J., Bruins, J., Glogger, M., Wilhelm, J., Frei, M.S., Tarnawski, M., D'Este, E., Heilemann, M., Hiblot, J., et al., "Exchangeable HaloTag Ligands for Super-Resolution Fluorescence Microscopy," Journal of the American Chemical Society 145(5), 3075–3083 (2023).
[16] Glogger, M., Wang, D., Kompa, J., Balakrishnan, A., Hiblot, J., Barth, H.-D., Johnsson, K., and Heilemann, M., "Synergizing Exchangeable Fluorophore Labels for Multitarget STED Microscopy," ACS nano 16(11), 17991–17997 (2022).
[17] Spahn, C., Grimm, J.B., Lavis, L.D., Lampe, M., and Heilemann, M., "Whole-Cell, 3D, and Multicolor STED Imaging with Exchangeable Fluorophores," Nano letters 19(1), 500–505 (2019).
[18] Jang, S., Narayanasamy, K.K., Rahm, J.V., Saguy, A., Kompa, J., Dietz, M.S., Johnsson, K., Shechtman, Y., and Heilemann, M., "Neural network-assisted single-molecule localization microscopy with a weak-affinity protein tag," Biophysical reports 3(3), 100123 (2023).
[19] Ebrahimi, V., Stephan, T., Kim, J., Carravilla, P., Eggeling, C., Jakobs, S., and Han, K.Y., "Deep learning enables fast, gentle STED microscopy," Communications biology 6(1), 674 (2023).
[20] Rahm, J.V., Balakrishnan, A., Wehrheim, M., Kaminer, A., Glogger, M., Kessler, L.F., Kaschube, M., Barth, H.-D., and Heilemann, M., "Fast and Long-Term Super-Resolution Imaging of Endoplasmic Reticulum Nano-structural Dynamics in Living Cells Using a Neural Network," Small Science2400385 (2024).
[21] Stepp, W.L., Durmus, E.B., Alvarez, S.N.R., Landoni, J.C., Tortarolo, G., Douglass, K.M., Weigert, M., and Manley, S., "Smart hybrid microscopy for cell-friendly detection of rare events," in bioRxiv (2025).
[22] Spahn, C., Endesfelder, U., and Heilemann, M., "Super-resolution imaging of Escherichia coli nucleoids reveals highly structured and asymmetric segregation during fast growth," Journal of structural biology 185(3), 243–249 (2014).
[23] Spahn, C., Middlemiss, S., Gómez-de-Mariscal, E., Henriques, R., Bode, H.B., Holden, S., and Heilemann, M., "The nucleoid of rapidly growing Escherichia coli localizes close to the inner membrane and is organized by transcription, translation, and cell geometry," Nature communications 16(1), 3732 (2025).
[24] Müller, B., and Heilemann, M., "Shedding new light on viruses: super-resolution microscopy for studying human immunodeficiency virus," Trends in microbiology 21(10), 522–533 (2013).
[25] Li, Y., Dietz, M.S., Barth, H.-D., Niemann, H.H., and Heilemann, M., "Single-Molecule FRET-Tracking of InlB-Activated MET Receptors in Living Cells," Small (Weinheim an der Bergstrasse, Germany)e07115 (2025).
[26] Li, Y., Arghittu, S.M., Dietz, M.S., Hella, G.J., Haße, D., Ferraris, D.M., Freund, P., Barth, H.-D., Iamele, L., et al., "Single-molecule imaging and molecular dynamics simulations reveal early activation of the MET receptor in

cells," Nature communications 15(1), 9486 (2024).